# High-spin states in $^{203}$Rn

H. Newman,[1,2] J. R. Novak,[1] C. W. Beausang,[1] C. J. Barton,[1] M. A. Caprio,[1] R. F. Casten,[1] J. R. Cooper,[1] A. A. Hecht,[1] R. Krücken,[1] N. Pietralla,[1] A. Wolf,[1,3,4] N. V. Zamfir,[1,3] Jing-ye Zhang,[1,5] K. E. Zyromski,[1] I. Birriel,[6] and J. Saladin[6]

[1]*Wright Nuclear Structure Laboratory, Yale University, New Haven, Connecticut 06520*

[2]*University of Surrey, Guildford, Surrey GU2 7XH, United Kingdom*

[3]*Clark University, Worcester, Massachusetts 01610*

[4]*Negev Research Center, Beer-Sheva 84750, Israel*

[5]*University of Tennessee, Knoxville, Tennessee 37996*

[6]*University of Pittsburgh, Pittsburgh, Pennsylvania 15260*

(Received 21 December 2000; published 13 July 2001)

The high-spin structure of $^{203}$Rn has been investigated using two separate reactions. $\gamma-\gamma$ coincidences were measured for the $^{174}$Yb($^{34}$S,5$n$) reaction at a beam energy of 167 MeV using the YRAST Ball array at the Wright Nuclear Structure Laboratory at Yale University. The $^{168}$Er($^{40}$Ar,5$n$) reaction at an energy of 188 MeV was also employed. In this experiment $\gamma$ rays were observed using the Gammasphere array in coincidence with the fragment mass analyzer at Argonne National Laboratory. The level scheme of $^{203}$Rn has been developed to spins of $\sim 41/2\hbar$ and excitation energies of $\sim 3$ MeV. The high-spin decay is dominated by three sequences of $\gamma$ rays, and the possible configurations are discussed.

DOI: 10.1103/PhysRevC.64.027304 PACS number(s): 23.20.Lv, 25.70.Gh, 27.80.+w

Nuclei lying near the doubly magic $^{208}$Pb have spherical ground states and their low-lying excitations are dominated by a variety of single-particle excitations. However, at higher spins and excitation energies, a variety of interesting collective phenomena are both predicted and observed. A striking example is the observation of superdeformed states in Hg, Tl, and Pb nuclei [1]. In these nuclei, favorable shell effects combined with the large Coulomb energy and reduced fission barrier serve to stabilize the superdeformed minimum down to fairly low-spin values. Indeed, superdeformation has been observed in $^{198}$Po [2] and superdeformed minima are predicted to occur for even heavier $Z$ nuclei. Another collective phenomenon found in this region is shears bands. These bands consist of long, regular cascades of stretched magnetic dipole transitions, and are well established in several Pb and Bi nuclei [1,3,4]. They should also occur in heavier nuclei. Recently a candidate shears band was reported in $^{205}$Rn [5].

Despite these interesting structural features, very little information is available on the excited states of odd or doubly odd nuclei in this region. The present paper concentrates on $^{203}$Rn, ($Z=86,N=117$). Previous in-beam work that had primarily focused on the neighboring even-even nucleus $^{202}$Rn had identified some preliminary candidates for $\gamma$-ray transitions in $^{203}$Rn [6], although no level scheme was reported. Alpha-decay spectroscopy and regional systematics give the ground-state spin and parity assignment of $^{203}$Rn as either $(3/2)^-$ or $(5/2)^-$ [7] with an excited $(13/2)^+$ level at 361 keV. In addition, if the ground state is $(3/2)^-$ then there is another excited level at 50 keV $(5/2)^-$.

Two experiments were performed to populate high-spin states in $^{203}$Rn. The first, carried out at the Wright Nuclear Structure Laboratory at Yale University, utilized the $^{174}$Yb($^{34}$S,5$n$) reaction at a beam energy of 167 MeV. An 800 $\mu$g/cm$^2$ target was used and decay $\gamma$ rays were measured using the YRAST Ball array [8]. At the time of this experiment the YRAST Ball consisted of 18 Compton suppressed Ge detectors and three large (each of $\sim$150% relative efficiency) suppressed segmented clover detectors [9], giving a total photopeak array efficiency of about 1.5%. A total of $5.0\times10^8$ two and higherfold coincidence events were recorded, which when unfolded resulted in a total of $6.0\times10^8$ $\gamma$-$\gamma$ coincidences.

The second experiment utilized the $^{168}$Er($^{40}$Ar,5$n$) reaction at a beam energy of 188 MeV, the beam being provided by the Argonne National Laboratory ATLAS accelerator. The Gammasphere array [10], which at the time consisted of 101 large volume Ge detectors, was used to record multiple $\gamma-\gamma$ coincident events, which were also tagged by evaporation residues detected using the Argonne fragment mass analyzer (FMA) [11]. A total of $1.2\times10^8$ $\gamma$-$\gamma$-$\gamma$ coincidences and $\sim10^4$ $\gamma$-recoil events were measured during a run time of approximately 24 h.

The study of $\gamma$-ray transitions between excited states in $^{203}$Rn is severely hampered by the presence of a very large background of $\gamma$ radiation from the decay of fission fragments and, in these reactions, also by a large flux of $\gamma$ rays associated with Coulomb excitation of the target nuclei. The total fission cross sections were calculated using PACE [12], and found to be 332 mb and 357 mb for the $^{34}$S+$^{174}$Yb and $^{40}$Ar+$^{168}$Er reactions, respectively. As a comparison, the estimated cross sections for $^{203}$Rn were 3.5 and 3.4 mb. In addition, higher spin states are much more likely to fission for the more symmetric Ar + Er reaction compared to the S + Yb reaction. This means that the high-spin survival probability for the sulfur reaction was greater, while the background was slightly less. Hence, the level scheme of $^{203}$Rn was deduced mainly from the $\gamma-\gamma$ coincidence data from the YRAST Ball data set while the high quality $\gamma$-recoil FMA data was valuable in the verification of new transitions in $^{203}$Rn, as were coincidences with radon x rays. The level scheme of $^{203}$Rn from the present paper is shown in Fig. 1. As can be seen, the decay is dominated by three cascades, labeled 1, 2, and 3 in Fig. 1. Spin and parity assignments are

 

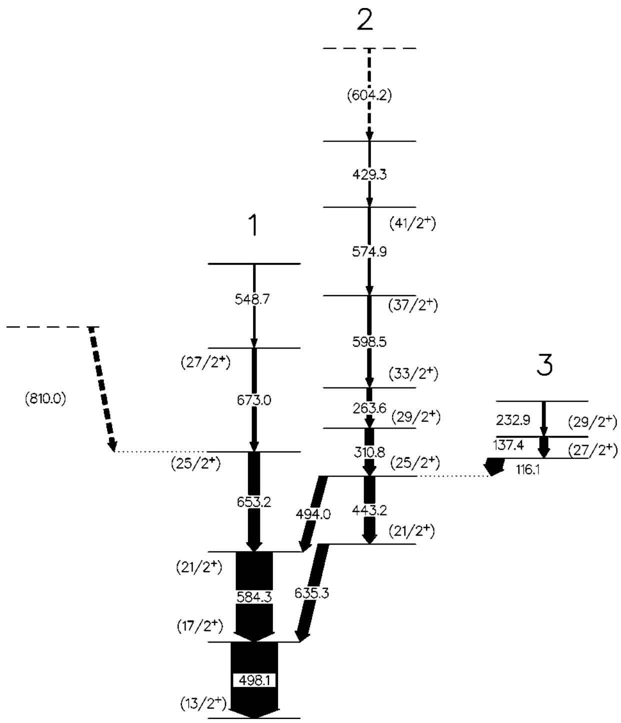


FIG. 1. Level scheme of $^{203}$Rn. Energies are in keV. Intensities, corrected for internal conversion, greater than 10% of the 498.1 keV $\frac{17}{2}\rightarrow\frac{13}{2}$ transition are indicated by proportionately broadened arrows. All spin and parity assignments are tentative. Tentative transitions are shown by dotted lines.

tentative and are based on both angular distribution arguments and polarization results. Our results for $^{203}$Rn are summarized in Table I and will be discussed in more detail below. To illustrate the quality of the data, a $\gamma-\gamma$ coincidence spectrum gated by the 498.1 keV transition and a spectrum gated by mass for recoils in the FMA are presented in Fig. 2.

To obtain information on the spins and parities of excited states in $^{203}$Rn, the angular properties of the gamma-ray transitions were measured. However, due to the small fusion probability and the large fission cross section encountered in these reactions, the gamma-ray angular distribution could not be measured in a singles spectrum. Furthermore, the available statistics did not allow for a complete angular correlation analysis to be carried out. Therefore, a gated angular distribution analysis was performed to assign transition multipolarities and spins. Matrices were constructed of $E_\gamma$(any) vs $E_\gamma(\theta)$, where "any" refers to any of the YRAST Ball detector angles ($\theta=50°$, 90°, 126°, and 160°) and $\theta$ to a specific angle with respect to the beam direction. Gates were then placed on the "any" axis and the intensity of the coincident gamma rays were measured as a function of angle with respect to the beam direction. Intensities were efficiency corrected, normalized to the 50° ring, and fitted to the function $I(\theta)=I_0\{1+a_2P_2[\cos(\theta)]\}$. A higher-order fit was not possible due to the small number of detector rings. $a_2$ coefficients were extracted for the majority of transitions and, assuming a stretched dipole or quadrupole character, this enabled their multipolarity to be assigned. The validity of such

TABLE I. The $\gamma$-ray energies, intensities, angular distribution, and polarization results, and multipolarity assignments for transitions in $^{203}$Rn.

| $E_\gamma$(keV) | Intensity [a] | $a_2$ [b] | $A$ [c] | Assignment |
|---|---|---|---|---|
| 116.2(5) | 36(9) | −0.4(1) | | $M1$ |
| 137.4(5) | 16(7) | −0.6(2) | | $M1$ |
| 232.9(1) | 5(2) | | | |
| 263.6(5) | 10(2) | 0.6(3) | | $E2$ |
| 310.8(1) | 19(3) | 0.7(1) | | $E2$ |
| 429.3(2) | | | | |
| 443.2(2) | 21(4) | 0.7(1) | | $E2$ |
| 494.0(1) | 18(3) | 0.3(2) | +0.2(2) | $E2$ |
| 498.1(1) | 100(8) | 0.8(5) | +0.2(1) | $E2$ |
| 548.6(5) | | | | |
| 574.9(1) | 5(2) | 0.9(4) | | $E2$ |
| 584.3(1) | 78(6) | 0.4(1) | +0.2(1) | $E2$ |
| 598.5(1) | 7(2) | 1.2(4) | | $E2$ |
| 604.2(5) | | | | |
| 635.3(1) | 23(3) | 0.4(1) | | $E2$ |
| 653.2(1) | 24(4) | 0.4(1) | $>0$ | $E2$ |
| 673.1(5) | 9(2) | -0.5(4) | | $M1$ |
| 810.5(5) | 15(3) | | | |

[a]Total intensity, corrected for internal conversion and normalized to the 498.1 keV transition.
[b]As extracted from a fit to $I(\theta)=I_0\{1+a_2P_2[\cos(\theta)]\}$.
[c]Defined as the ratio $(N_\perp-N_\parallel)/(N_\perp+N_\parallel)$, where $N_\perp$ is the number of clover-addback counts due to Compton scattering at 90° with respect to the reaction plane, and $N_\parallel$ is that due to scattering parallel to the reaction plane.

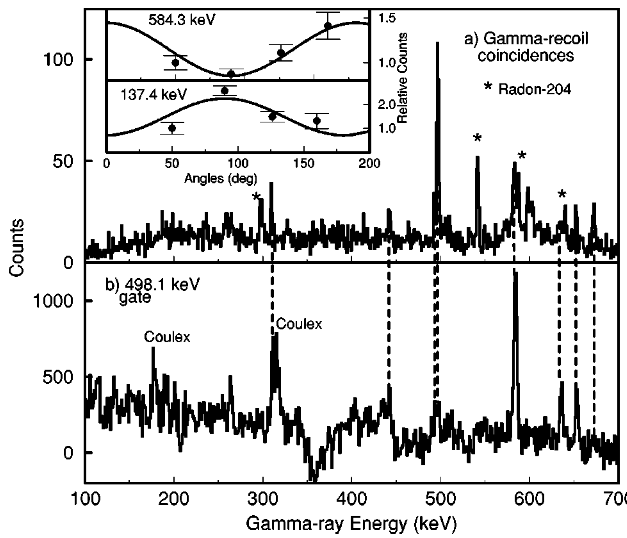


FIG. 2. (a) $\gamma$ rays in coincidence with evaporation residues detected in the FMA. (b) Spectrum of $\gamma$ rays in coincidence with the 498.1 keV transition in $^{203}$Rn. In both spectra the main $^{203}$Rn peaks are shown by the dashed lines. The inset shows examples of angular distribution results.

an analysis was checked by measuring known stretched $E2$ and $E1$ transitions in the neighboring even-even nucleus $^{206}$Rn. Stretched $E2$ transitions yielded a positive and $E1$ a negative $a_2$. The results from this analysis for $^{203}$Rn are summarized in Table I.

To determine the electric or magnetic character of the transitions, the clover detectors situated at 90° in the YRAST Ball were used as in-beam Compton polarimeters [9]. At this angle, the polarization is directly proportional to the experimental asymmetry, which is defined as the ratio: $A=(N_{\perp}-N_{\parallel})/(N_{\perp}+N_{\parallel})$, where $N_{\perp}$ is the number of clover-addback counts due to Compton scattering at 90° with respect to the reaction plane, and $N_{\parallel}$ is that due to scattering parallel to the reaction plane. A positive value for the asymmetry at an observation angle of 90° relative to the beam axis is indicative of an electric transition, while a negative value signifies a magnetic transition. The asymmetry $A$ was measured for four transitions in $^{203}$Rn. Each resulted in a positive value leading to an electric assignment. Combined with the positive $a_2$ values obtained from the angular distribution analysis, these transitions are assigned as stretched $E2$. The results of this polarization analysis are summarized in Table I.

With 86 protons and 117 neutrons, $^{203}$Rn lies close to the closed shells of 82 and 126 and to the doubly magic nucleus, $^{208}$Pb. The nearby high-$j$ orbitals available for the four valence protons are $h_{9/2}$, $f_{7/2}$ and $i_{13/2}$. Likewise, the single-particle neutron holes close to the Fermi surface include the $f_{5/2}$ and $i_{13/2}$ orbitals.

Previous studies of $^{203}$Rn indicate the presence of a $13/2^+$ state at an excitation energy of about 360 keV [7]. It is not possible to detect $\gamma$ rays deexciting this level as its lifetime is $\sim$28 s [7]. Since heavy-ion fusion-evaporation reactions preferentially populate high-$j$ states, it is natural to associate the bandhead of cascade 1 with this state, leading to a spin, parity assignment of $13/2^+$ and a $\nu i_{13/2}^{-1}$ configuration. Total Routhian surface calculations using the ultimate cranker [13] indicate that the $\nu i_{13/2}^{-1}$ configuration is indeed low lying and predict a small oblate deformation of $\epsilon\sim-0.13$. The cascade built on the $(13/2^+)$ state is therefore considered to be the $i_{13/2}$ neutron hole coupled to the even-even core. The 673 keV transition near the top of this sequence has a negative $a_2$ coefficient, implying a dipole character. This may indicate a change in configuration at this point in the cascade. However, more statistics are needed to clarify this point.

The configuration of the second cascade, labeled 2 in Fig. 1, is not completely clear. It is connected to the low-lying yrast states by the 494 and 635 keV linking transitions, both of which have large positive $a_2$ coefficients and are assigned as stretched $E2$ transitions. While nonstretched $J\rightarrow J$ dipole transitions can also have large positive $a_2$ coefficients, a stretched $E2$ assignment is considered more likely due to the intensity pattern, which implies that cascade 2 becomes yrast. Thus it is assigned the same parity (positive) as cascade 1. Comparisons with the neighboring even-even nuclei shows that the $\pi h_{9/2}^2$ states feature strongly and lead to the presence of $J^{\pi}=8^+$ isomers in these nuclei. This feature has not been seen in either $^{203}$Rn or $^{205}$Rn, and would lead us to propose that the $\pi h_{9/2}^2$ configuration is not prominent in these odd radon nuclei. It was found that with decreasing neutron number and increasing collectivity, the $f_{7/2}^2$ proton configuration is especially likely [14]. Thus $\pi f_{7/2}^2 \otimes \nu i_{13/2}^{-1}$ is certainly a good candidate for the configuration of the second cascade as is $\nu(f_{5/2}^{-2} i_{13/2}^{-1})$. At this stage it is felt that either configuration is plausible.

Cascade 3 currently has only three transitions, two of which have been identified as dipole in character while the third one remains unassigned. It is possible that this is the start of a magnetic dipole band, similar to that seen in $^{205}$Rn [5], although more lifetime information and transitions are needed to test this hypothesis.

In conclusion, the high-spin level scheme of $^{203}$Rn has been investigated for the first time. Two cascades dominate the decay, while a shorter third one is also present. The first is assigned to the $\nu i_{13/2}^{-1}$ configuration and consists of one $M1$ and four $E2$ transitions. The second band consists of seven transitions, five of which have been given an $E2$ assignment. These two bands are connected by two $E2$ transitions, implying that they have the same parity. The third, less intense, cascade currently has two $M1$ assigned transitions and one unassigned one. All multipolarity assignments are on the basis of observed Compton asymmetries and angular distribution patterns.

The authors would like to gratefully acknowledge the ATLAS support staff at Argonne National Laboratory and the staff at the Wright Nuclear Structure Laboratory for supplying the beams. Special thanks is also extended to the Gammasphere support staff, especially, M. P. Carpenter, R. V. F. Janssens, F. Kondev, C. J. Lister, D. Seweryniak, and I. Wiedenhoever, for their invaluable assistance and help during our experiment. This work was partly supported by the U.S. DOE Grant Nos. DE-FG02-91ER-40609, DE-FG02-88ER-40417, DE-FG05-96ER-40983, and by the DFG under Contract No. Pi393/1-1.

[1] R. M. Clark *et al.*, Phys. Rev. Lett. **78**, 1868 (1997); Nucl. Phys. **A562**, 121 (1993).
[2] D. P. McNabb *et al.*, Phys. Rev. C **53**, R541 (1996).
[3] S. Frauendorf, Nucl. Phys. **A557**, 259 (1993).
[4] G. Baldsiefen *et al.*, Nucl. Phys. **A574**, 521 (1994); **A592**, 365 (1995); Phys. Rev. C **54**, 1106 (1996).
[5] J. R. Novak *et al.*, Phys. Rev. C **59**, R2989 (1999).
[6] S. J. Freeman *et al.*, Phys. Rev. C **50**, 1754 (1994).
[7] S. Rab, Nucl. Data Sheets **70**, 173 (1993).
[8] C. W. Beausang *et al.*, Nucl. Instrum. Methods Res. A **452**, 431 (2000).
[9] G. Duchêne, F. A. Beck, D. Curien, G. de France, L. Han, C. W. Beausang, M. A. Bentley, P. J. Nolan, J. Simpson, and P. J. Twin, Nucl. Instrum. Methods Phys. Rev. A **432**, 90 (1999).
[10] P. J. Nolan, F. A. Beck, and D. B. Fossan, Annu. Rev. Nucl. Part. Sci. **45**, 561 (1994).
[11] C. N. Davids and J. D. Larson, Nucl. Instrum. Methods Phys. Rev. B **40/41**, 1224 (1989); C. N. Davids, B. B. Buck, K. Bindra, D. J. Henderson, W. Kutschere, T. Lauritsen, Y. Nagame, P. Sugathan, A. V. Ramayya, and W. B. Walters, *ibid.* **70**, 358 (1992).
[12] A. Gavron, Phys. Rev. C **21**, 230 (1980).
[13] T. Bengtsson, Nucl. Phys. **A496**, 56 (1989).
[14] D. Horn, C. Baktash, and C. J. Lister, Phys. Rev. C **24**, 2136 (1981).